Instituto Nacional de Astrofísica, Optica y Electrónica.

REPORTE TECNICO

COORDINACION DE ÓPTICA

Ray and wave optics relation in nearly regular resonators

N.Korneev

No.639

Ray and wave optics relation in nearly regular resonators

N.Korneev

December 5, 2016

0.1 General

This report is the extended version of the paper [1]. It includes the material which did not enter the final version of the paper because of the size limitations, as well as extended discussion and introduction part.

0.2 Introduction

In optics, two-dimensional cavity is formed by a region of a plane bounded by a closed curve. Classically, the ray is reflected from the boundary according to the law of specular reflection, and the trajectory is composed by an infinite number of straight line segments between reflections. For the wave description, the Helmholtz equation with appropriate boundary condition is solved. Though we mostly use optical language here, the situation is mathematically equivalent to the transition from classical to quantum mechanics for a free movement of a particle in a closed 2D region of space with a boundary (classical or quantum billiard)[2].

Billiards are simple, but important mechanical systems which can demonstrate very complicated behaviour if the billiard boundary is not regular. We mean by regular shape the one, for which simple exact solution of a billiard problem exists. Particular cases of regular billiards are rectangular, circular and elliptic, for which additional integrals of motion can be found and it is possible to obtain action-angle variables in a closed form. For rectangular billiard, momentum projections to coordinate axes are conserved (except for changing sign). For a circular billiard the angular momentum with respect to the circle center, and for the elliptic case the product of two angular momenta with respect to the ellipse foci are conserved. The existence of such conserved quantities according to rather general theorems of mechanics mean, that the Hamiltonian of a system can be written as a function of two actions, the motion is periodic and characterized by two frequencies, and the trajectories in a phase space lie on invariant tori.

The quantum billiard corresponds to the transition from classical to quantum mechanics, and mathematically it is equivalent to finding a mode structure of the corresponding cavity. The problem, apart from theoretical interest [2], has important applications for the calculation of modal structure for laser microcavities [3, 4], which is notoriously difficult task even with the numerical methods.

For illustration, let us consider the circular resonator with a unity radius (Fig.1). The classical trajectory for it is shown by lines. It is seen, that the distance ρ, or the characteristic angle γ_0 is the same after reflection. The trajectory form a caustic at a distance ρ from the centre. If the angle γ_0 is such, that the trajectory is periodic, there is no complete caustic, but it is formed if we take all periodic trajectories with the same angle γ_0 and different initial points. In terms of invariant tori is means that the torus in question is separated into an infinite number of trajectories, and not covered completely by a single trajectory with an irrational winding number.

In a case of circle it is rather easy to establish a correspondence between the classical description and wave optics. The solution of Helmholtz equation in the circle is given by the product of sine/cosine function of the angle $\sin(\phi)$,$\cos(\phi)$

and the Bessel function $J_n(a_{n,p}r)$ of distance from center r. For large n, the Bessel function has a characteristic maximal value, which corresponds to a classical caustic.

However, even small shape perturbation from a regular case result for trajectories in a very complicated behaviour called Kolmogorov-Arnold-Moser (KAM) chaos [1,2]. Under smooth small distortion of resonator shape, most trajectories remain qualitatively similar. However, the trajectories close to periodic ones for a circle split and finally form a chaotic region in the phase space. For a weak chaos the trajectories form in a phase space characteristic structures. We are interested here to investigate the resonator modes, which correspond to such structures. For this it is reasonable to use a perturbation theory with a shape distortion as a small parameter.

Perturbation methods to obtain approximations for shapes, which are close to solvable ones [5, 6, 7] are known, but these methods are effective only when $d \sim K^{-2}/L$, where d is a typical shape distortion (e.g. the distance between undistorted and distorted boundary), L is a typical length (e.g. diameter of a circle), and K is a wavevector of a mode ($-K^2$ is an eigenvalue of Laplace operator). Thus, those methods are not efficient for big K. On the other hand, semiclassical approximations exist, which are valid for big K numbers, but only for the cases when classical ray trajectories in a resonator are not chaotic or unstable. In particular, efficient approximations can be obtained for resonator modes corresponding to classically stable periodic ray trajectories [8].

We combine the two approaches, and develop a perturbation method, which works for higher modes *and* nearly regular cavity up to the next perturbation scale, $d \sim K^{-1}$.

The method implementation is based on two observations. First, in a semiclassical limit of big K the eigenvalue structure for a regular cavity demonstrates special features, 'arcs', corresponding to periodic ray trajectories. Second, for a wide class of smooth shape distortions, the perturbation matrix, limited to modes within an arc, has simple universal structure, and the resulting problem can be solved in terms of solutions of Hill equation, and for some particular cases, of Mathieu equation. The modes, which are thus obtained, include the Hermite-Gauss modes, the slightly distorted modes of a regular cavity, such as whispering gallery modes, and modes approximately corresponding to unstable periodic trajectories, scar modes in particular. Most of them are expressed as a superposition of many modes of unperturbed cavity with comparable coefficients, and cannot be considered as a small perturbation of a single mode of regular cavity.

Establishing the relation between ray and wave description (or, equivalently, between classical and quantum mechanics in billiard) for the initial stage of KAM chaos is an interesting theoretical question. This relation can also be useful for practical calculations in different types of resonators in optics, microwave, acoustics etc., since, as we show below, the numerics for resulting approximations can be easier, than for the full solution.

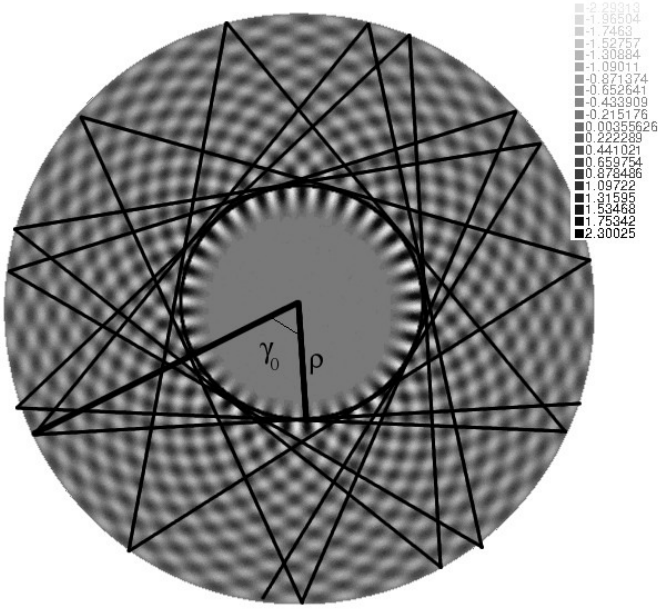

Figure 1: The relation between the real part of cylindrical harmonic Eq.(8) (grayscale) and ray trajectory (thin lines) in a unit circle. The trajectory is defined by the angle γ_0, or equivalently by the caustic radius ρ. In terms of large order Bessel functions, $cos(\gamma_0) \approx n/a_{n,p} = \rho$, since the geometric caustic corresponds to the place, where argument of Bessel function is approximately equal to its order.

0.3 Conformal mapping and perturbation operator

The usual approach to obtain perturbation matrix for slightly deformed resonator is based on the Hadamard formula for Green function of a perturbed domain [6, 5]. For two dimensions, another possible method is conformal mapping. Though conformal maps are common for solving the Laplace equation, their application to Helmholtz equation is not very frequent. Some classic applications are reviewed in Ref.[9], for recent papers see e.g. [10, 11]. The idea of the method is that if an analytic function of complex variable, $w(z)$ maps a simple shape (circle, rectangle, etc.), to a cavity boundary, the solution of Helmholtz equation in a resonator with complicated boundary is mapped to a solution for a resonator with a simple form filled with a medium which has effective refractive index distribution depending on $|w'(z)|^2$. If the distortion of regular shape is small, perturbation approach can be used to obtain approximations to new modes in a form of superposition of eigenfunctions of unperturbed problem.

Consider an analytic function $w(z) = u(z) + iv(z)$ of $z = x + iy$ with values in a region having a boundary Γ. Consider the real function $f(u, v)$ which is zero on Γ (Dirichlet boundary condition) and obeys the Helmholtz equation:

$$- \triangle_{u,v} f = \mu f, \tag{1}$$

with a Laplace operator $\triangle_{u,v} = \partial_u^2 + \partial_v^2$. If Γ is an image of a regular domain boundary S upon $w(z)$, then $f(x,y) = f(w(z))$ is a function on a regular domain, which has zero value on a boundary S, and the Eq.(1) in new variables becomes:

$$-\triangle_{x,y} f(w(x,y)) = \mu f |w'(z)|^2. \tag{2}$$

The approximation we are interested in is obtained for a small distortion of a shape, i.e. function $w(z)$ is

$$w(z) = z + d(z), \tag{3}$$

with a small addition $|d(z)| \ll z, |d'(z)| \ll 1$. If we consider eigenfunctions having eigenvalues close to a big number μ^0, such as $|\mu^0 - \mu| \ll \mu^0$, we can expand the right-hand side of Eq.(2), to the first order in d' and $\mu^0 - \mu$, which gives a self-adjoint Schrödinger type spectral problem on a regular domain:

$$-\triangle_{x,y} f(x,y) - 2\mu^0 Re[d'(z)] f(x,y) = \mu f(x,y). \tag{4}$$

In this case, the unperturbed operator is simply a Laplace operator $A^0 f = -\triangle f$ with known eigenfunctions $f^0_{n,p}$ and eigenvalues $\mu^0_{n,p}$. The perturbation operator P is multiplication by a function: $Pf = -2\mu^0 Re[d'(z)]f$.

The perturbation theory for the Schrödinger operator is well known in quantum mechanics. According to the Weyl's theorem, the average distance between Laplace operator eigenvalues for a 2D domain is $4\pi/\Omega$, where $\Omega = L^2$ is the domain area, and L its characteristic length. From the Eq.(3), the characteristic displacement of the boundary under perturbation is d, and the characteristic derivative value is d/L. The simple perturbation methods work for perturbation strength smaller than a distance between levels, which gives usual $2\mu^0 d/L \sim 4\pi/L^2$, or $d \sim K^{-2}/L$ estimation of the Introduction.

The perturbation theory in the above mentioned sense can be built for a small distortion of any domain, for which Laplace equation eigenfunctions are known. However, as it is discussed in the next section, simple domains, for which analytic solutions exist, have special spectral structures, corresponding for a semiclassical regime to periodic ray trajectories, and in this case perturbation problem can be approximately solved in special functions for $d \sim K^{-1}$.

0.4 Perturbation for regular cavities

The Laplace operator can be regarded as a quantization of Hamiltonian task of a classical movement of a free particle in a billiard, which has a shape of the cavity [2]. If the classical Hamiltonian problem is integrable, action-angle variables exist, and the Hamiltonian is a function of two actions $H(I_1, I_2)$. For the semiclassical approximation, energies (mode eigenvalues) in this case are obtained by setting $I_{1,2} = q_{1,2} + \frac{1}{4}\alpha_{1,2}$, where $q_{1,2}$ are integer mode numbers, and $\alpha_{1,2}$ are fixed integers, depending on the properties of the trajectory (Maslov indices)[12, 13]. These points locally form a square lattice in a plane I_1, I_2. The typical case is shown in Fig.1.

Let us fix a line in the lattice, parallel to $(m, -l)$ vector. Consider the situation when it is tangent to the Hamiltonian level line $H(I_1, I_2) = const$, and m, l are small co-prime integers. Fix local coordinates n_1, n_2 with the

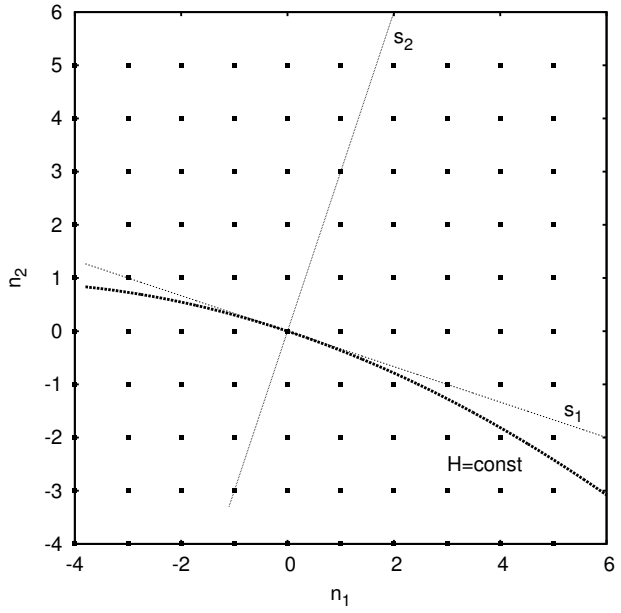

Figure 2: A small part of plane of action variables I_1, I_2. The line $H = const$ is tangent to a new coordinate axis s_1. For this plot $m = 3, l = 1$.

origin in a lattice point close to the contact point. Now introduce another set of coordinates in a plane by:

$$s_1 = mn_1 - ln_2 \tag{5}$$

$$s_2 = ln_1 + mn_2. \tag{6}$$

This transformation is equivalent to a rotation and changing a scale by $\sqrt{m^2 + l^2}$ factor. Both s_1 and s_2 are integer, but they do not change independently. The lattice in new coordinates consists in repeating an elementary unit with $m^2 + l^2$ length in two directions. For lattice points, we obtain rows for all integer s_2. In each row, s_1 coordinate changes by $m^2 + l^2$ from point to point. To obtain the relative shift of the points in two consecutive rows, it is necessary to solve the Diophantine equation.

For big mode numbers q_1, q_2, the curvature of Hamiltonian level lines becomes small, and the energy in new coordinates is expressed to the lowest order in $s_{1,2}$ by:

$$\mu(s_1, s_2) = \mu_0 + \alpha_1(s_1 - \delta_H)^2 + \alpha_2 s_2, \tag{7}$$

where the relation $\alpha_2 \gg \alpha_1$ holds. This gives characteristic arcs in dependence of eigenvalues on the mode number n_1. The condition that tangent to a level line is parallel to a $(m, -l)$ vector is equivalent to that one of Hamiltonian gradient parallel to (l, m) vector, and this means, that corresponding classical trajectory is periodic [12]. Illustrations for particular cases are given in following sections (see Figs.5,7).

Since in the semiclassical region the energy difference between consecutive arcs is much bigger, than the typical energy difference within a single arc, the

perturbation, if it is small enough, can be limited to one arc. The energy difference between arcs scales as $\sqrt{\mu}$, and thus the perturbation scale is $d \sim K^{-1}$.

If $f_{q1,q2}$ are eigenfunctions of Laplace operator in a regular domain, we fix a set of modes with the same s_2:

$$b_k(x,y) = f_{q1+km,q2-kl}(x,y). \tag{8}$$

The Laplace operator limited to this set is diagonal

$$\langle b_k| - \triangle |b_k\rangle = \mu^0 + \alpha(k-\delta)^2, \tag{9}$$

and $\delta = \delta_H + \delta_{s2}$ is a phase which depends on s_2 value. It can be taken $0 \leqslant \delta < 1$ by shifting the origin. The perturbation matrix elements between $b_{k_1}, b_{k_2}$for semiclassical regime depend to the first approximation on the difference $|k_1 - k_2|$ only. This is related to the fact, that in a semiclassical regime the eigenfunctions are represented as rapidly varying cosine functions with slowly varying amplitude and phase (we consider the examples below). Thus, when k_1, k_2 are much smaller, than q_1, q_2:

$$\langle b_{k_1}|P|b_{k_2}\rangle \sim P_{|k_1-k_2|}. \tag{10}$$

This gives approximately diagonal-constant symmetric perturbation matrix. The eigenfunction is

$$g(x,y) = \sum_{k=-\infty}^{\infty} \psi_k b_k(x,y), \tag{11}$$

where ψ_k are components of eigenvecotr for the infinite matrix given by Eqs.(9,10). Consider a generating function expressed by a Fourier series with the eigenvector components:

$$G(\nu) = \exp(-i\delta\nu) \sum_{k=-\infty}^{\infty} \psi_k exp(ik\nu). \tag{12}$$

The action of a matrix on ψ_k is equivalent to the action on $G(\nu)$ of the operator

$$\mu^0 - \alpha \frac{d^2}{d\nu^2} + P(\nu), \tag{13}$$

where

$$P(\nu) = P_0 + 2\sum_{q=1}^{\infty} P_q \cos(q\nu). \tag{14}$$

is a 2π-periodic function. Together with a boundary condition, that $G(\nu+2\pi) = G(\nu)\exp(-i2\pi\delta)$ this gives a spectral problem for the Hill equation, and it is physically equivalent to Schrödinger equation in periodic 1D potential.

In the simplest case, which is easily realized for square and circle, only $P_1 \neq 0$, and Hill equation is reduced to Mathieu equation:

$$-\frac{d^2}{d\nu^2}G(\nu) + 2d\cos(\nu)G(\nu) = \lambda G(\nu), \tag{15}$$

where $d = P_1/\alpha$, and λ is a rescaled eigenvalue $\lambda = (\mu - \mu^0)/\alpha$.

For big $|d|$, the equation can be studied in WKB approximation. Consider first $\delta = 0$. Choose $-\pi < \nu < \pi$ range, and negative d. If $d > 0$ the solution is

obtained from the negative d case by taking $\nu - \pi$ instead of ν, and the spectrum remains unchanged. Then, for a symmetric function:

$$G(\nu) \sim (\lambda - 2d\cos(\nu))^{-\frac{1}{4}} \cos(\int_0^\nu \sqrt{\lambda - 2d\cos(x')}dx'), \tag{16}$$

and for antisymmetric one:

$$G(\nu) \sim (\lambda - 2d\cos(\nu))^{-\frac{1}{4}} \sin(\int_0^\nu \sqrt{\lambda - 2d\cos(x')}dx'), \tag{17}$$

These equations are valid between classical turning points, i.e when the expression under the square root is positive. When it is negative, the eigenfunction exponentially diminishes into classically prohibited region of ν.

The lowest eigenvalue is approximately $\lambda \simeq -|2d|$. For low eigenvalues, the cosine function around the minimum can be approximated by a parabola. This gives a quantum oscillator problem, which has a solution in Hermite functions, and equally spaced eigenvalues. The Fourier transform of the Hermite function is also the Hermite function, which gives ψ_k values. If $\lambda \gg |2d|$, the solution is approximated by slightly perturbed sine/cosine function, and eigenvalue is proportional to a square of a mode number. Note, that for low eigenvalues and $\delta = 0$, consequent symmetric and antisymmetric eigenvectors have equally spaced eigenvalues, but for $\lambda \gg |2d|$ pairs are nearly degenerate. The level $\lambda \simeq |2d|$ separates these two regimes. Around this value, the distance between consequent eigenvalues diminishes. Note also, that the WKB approximation solution close to turning points behaves as $\delta\nu^{-\frac{1}{4}}$ if $\lambda < |2d|$, but as $\delta\nu^{-\frac{1}{2}}$ if $\lambda \sim |2d|$.

The approximate density of modes for eigenvalues around λ can be obtained using WKB method, and it is expressed in elliptic integrals:

$$f_-(\lambda) = \frac{1}{\pi\sqrt{|d|}} \int_0^1 \frac{ds}{\sqrt{(1-s^2)(1-q_-^2 s^2)}} = \frac{K(q_-)}{\pi\sqrt{|d|}}, \tag{18}$$

where $q_- = \sqrt{(2|d| + \lambda)/(4|d|)}$. For the case of $\lambda > 2|d|$, the same procedure gives

$$f_+(\lambda) = \frac{q_+ K(q_+)}{2\pi\sqrt{|d|}}, \tag{19}$$

with $q_+ = 1/q_-$, and an additional factor of 2 reflecting that now it is the difference between pairs of closely spaced eigenvalues is taken. The distance between consecutive eigenvalues in function of eigenvalue itself is then given by

$$\Delta\lambda(\lambda)_\pm = 1/f_\pm(\lambda). \tag{20}$$

These equations describe quite well numerical results (Fig.2b).

The behaviour of eigenvalues and eigenvectors ψ_k is shown in Figures 3 and 4. For these plots, the perturbation matrix of Eqs.(9,10) was taken, and its spectrum and eigenvectors were found by a standard numerical procedure. The physical meaning of the resonator mode corresponding to the solution is easier understood for a circular resonator, and it will be considered below.

If $\delta \neq 0$, the general character of spectrum is similar, but eigenvalues are no more nearly degenerate for $\lambda \gg 2|d|$. The case of a single coefficient P_q when

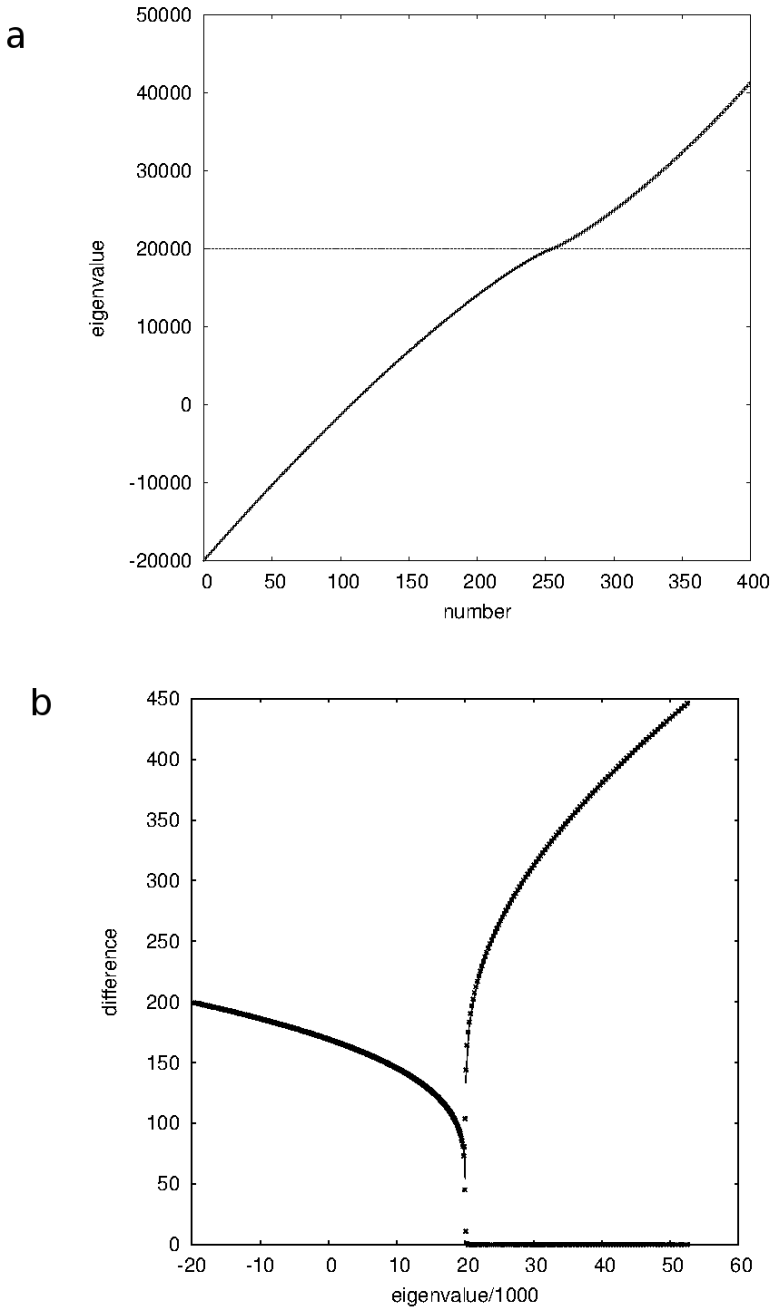

Figure 3: Numerically calculated eigenvalues of three-diagonal matrix A with $A_{k,k} = k^2$, and $A_{k,k\pm1} = d$ for $d = -10000$. The index range for calculation is $-500 \leqslant k \leqslant 500$. The approximate expressions of Eqs.(18,19) are shown in thin lines in plot (b).

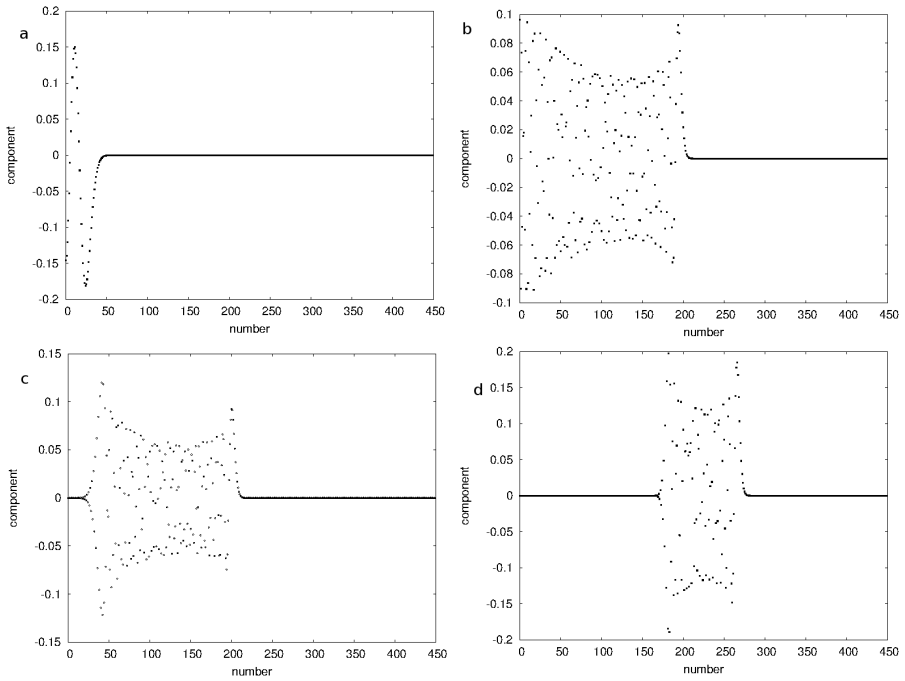

Figure 4: Calculated eigenvector components ψ_k for $d = -10000$ and different eigenvalue number N (see Fig.2a for corresponding eigenvalues). Since the eigenvectors are symmetric or antisymmetric, only positive k are shown. a) For $N = 4$, the eigenvector is approximately the fourth Hermite function b.) For $N = 240$ the eigenvector spreads to $k \approx 2\sqrt{d}$ c) For $N = 270$ the components for k close to zero become exponentially small. d) For $N = 451$ the eigenvector is localized far from zero.

$q \neq 1$ is reduced to the investigation of $G(\nu)$ over one period of $\cos(q\nu)$, and the solutions must have appropriate phase shift.

Smooth potentials $P(\nu)$, where P_q coefficients rapidly diminish in function of q will result in qualitatively similar behaviour which can be investigated by WKB approximation.

However, some distortions of boundary produce potentials which are not smooth. One case is when the right angle in the rectangle changes, or when the curvature of a smooth boundary becomes infinite under mapping - the conformal map then has a singularity. The spectral problem for one arc in this case can still be meaningful. However, the same point q_1, q_2 can be included in many arcs, most of them are characterized by big denominators m, and for approximation validity it is essential, that interaction within arcs having big m number is weak. This condition can break for slowly diminishing P_q, and it will be necessary to consider many arcs within one matrix. Such situation generally corresponds to developed chaos for ray trajectories, and it is not considered here.

Another problem exists if the trajectories have different topological properties, as it is observed for the ellipse [13, 14] . In this case, the phase space is divided into regions, where Maslov indices $\alpha_{1,2}$ are different. The lattice at boundary of the regions is not regular in this case, and the matrix of a perturbation that mixes states from both sides of the dividing line in the action space cannot be constructed with the outlined approach. It still works, however, in the regions of action plane far enough from such dividing lines.

0.5 Square cavity

For a square, calculations can be done explicitly. Take $0 < x \leqslant 1, 0 < y \leqslant 1$. The Hamiltonian (if mass is 1/2) is $H = p_x^2 + p_y^2$, with standard momenta. In function of two actions it is expressed as [15]:

$$H(I_x, I_y) = \pi^2(I_x^2 + I_y^2), \tag{21}$$

and the actions are proportional to absolute values of corresponding momenta $I_{x,y} = |p_{x,y}|/\pi$. The level lines are thus circles, the curvature is constant. The gradient vector is parallel to $(|p_x|, |p_y|)$, and the condition for periodic trajectory is $|p_x|m = |p_y|l$.

The Laplace operator eigenfunctions are given by

$$f_{q1,q2}(x, y) = 2\sin(\pi q_1 x)\sin(\pi q_2 y), \tag{22}$$

with $q_1, q_2 = 1, 2...$ Their eigenvalues for Eq.(1) are:

$$\mu(q_1, q_2) = \pi^2(q_1^2 + q_2^2). \tag{23}$$

Choose the origin in a point corresponding to a periodic trajectory: Q_1, Q_2, such that $Q_1 m = Q_2 l$. Then $q_{1,2} = Q_{1,2} + n_{1,2}$, and for the rotated coordinate system, given by Eqs(5,6), the Eq.(23) becomes:

$$\mu(s_1, s_2) = \mu^0 + \alpha_1(s_1^2 + s_2^2) + \alpha_2 s_2, \tag{24}$$

with $\mu^0 = \pi^2(Q_1^2 + Q_2^2)$, $\alpha_1 = \pi^2(m^2 + l^2)^{-1}$, and $\alpha_2 = 2\pi^2(m^2 + l^2)^{-1}(Q_1 l + Q_2 m)$. For big mode numbers $Q_{1,2}$, $\alpha_2 \sim \sqrt{\mu} \gg \alpha_1$, and by neglecting $\alpha_1 s_2^2$

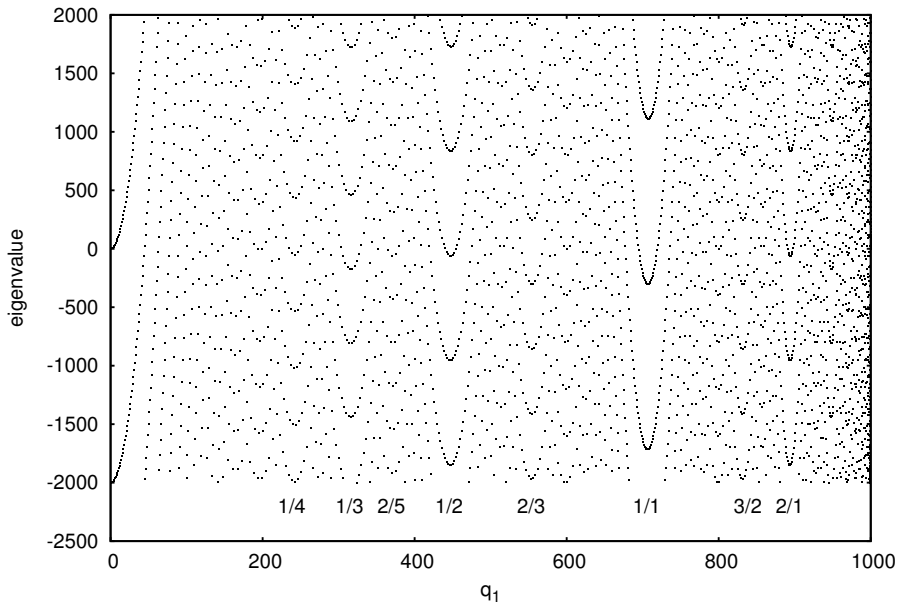

Figure 5: Square resonator eigenvalues, $(\mu - 10^6)/\pi^2$ in function of mode number q_1. The arc positions are given by a condition $q_1/1000 = l/\sqrt{l^2+m^2}$, and l/m values are marked for some of them.

term in comparison with $\alpha_2 s_2$ we obtain the form of Eq.(7). The eigenvalues Eq.(23) close to $\pi^2 10^6$ are shown in Fig.4. The arcs for small m, l are marked.

The conformal maps can be chosen as:

$$w(z) = z + d(z) = z + \sum_{m=1}^{\infty} c_m \sin(\pi m z), \tag{25}$$

where all c_m are real, and $|d'(z)| \ll 1$ inside the square. Then the square distortion under the conformal map is such, that $x = 0, x = 1, y = 0$ sides remain the same, but $y = 1$ side is transformed in a limit of small perturbation into the curve with equation

$$y(x) = 1 + \sum_{m=1}^{\infty} c_m \cos(\pi m x) \sinh(\pi m). \tag{26}$$

If only $c_1 \neq 0$, this is equivalent to one half of the ripple billiard [16]. Note, that conformal mapping preserves right angles, otherwise $w'(z) = 0$, or $w'(z) = \infty$ in the angle, and this needs a special consideration. If a small smooth boundary perturbation $y(x)$, which has $y'(0) = y'(1) = 0$ is given, it can always be expanded in a series Eq.(9).

The matrix elements of perturbation from the Eq.(4), which correspond to

only one term in Eq.(25) are then given by the integral over unit square

$$P_{n1,p1;n2,p2} = -2\mu^0 \pi m c_m \int \cos(\pi m x)\cosh(\pi m y) f_{n1,p1}(x,y) f_{n2,p2}(x,y) dxdy. \tag{27}$$

They are equal to

$$P_{n1,p1;n2,p2} = \mu^0 m^2 c_m (-1)^{q+1} \sinh(\pi m)(\frac{1}{m^2+q^2} - \frac{1}{m^2+(p_1+p_2)^2}), \tag{28}$$

if $n_1 = n_2 \pm m$, $n_{1,2} > m$, and $q = p_1 - p_2$. If $n_1 \neq n_2 \pm m$, the matrix element is zero.

Now, choose the mode which corresponds to a periodic trajectory with short period, such as n_0, p_0 are related as $n_0 m = p_0 l$ (m, l are small co-prime integers). Then select a subset of modes b_k, along s_1 axis, which passes through n_0, p_0 point. It is given by Eq.(8) with $q_1 = n_0, q_2 = p_0$

This corresponds to considering only one arc in Fig.4. It can be done, while $c_m \lesssim 1/\sqrt{\mu^0} \sim K^{-1}$, which means that perturbation is smaller, than a characteristic distance to the next arc. The diagonal matrix elements of Eq.(4), limited to b_k are:

$$\langle b_k| - \triangle |b_k\rangle = \pi^2(n_0^2 + p_0^2 + k^2(m^2+l^2)). \tag{29}$$

If we have only one term in the sum of Eq.(25) $c_m \neq 0$, the only non-zero off-diagonal elements are:

$$\langle b_s|P|b_{s\pm1}\rangle = \mu^0 m^2 c_m (-1)^{l+1} \sinh(\pi m)(\frac{1}{m^2+l^2} - \frac{1}{m^2+(2p_0 - l(2k+1))^2}). \tag{30}$$

If $p_0 \gg l(2k+1)$ this is reduced to

$$\langle b_k|P|b_{k\pm1}\rangle = \mu^0 m^2 c_m (-1)^{l+1} \sinh(\pi m)(\frac{1}{m^2+l^2} - \frac{1}{m^2+4p_0^2}) + \mathcal{O}(\frac{k}{p_0^3}). \tag{31}$$

Thus, the problem is reduced to the solution of Mathieu equation of previous section. The same procedure, with simple modifications, can be used for a rectangular cavity $0 < x < L_x, 0 < y < L_y$.

0.6 Circular cavity

Consider a unit radius circle, and cylindrical coordinates r, ϕ, such as $x = r\cos(\phi)$ and $y = r\sin(\phi)$, $0 \leqslant r \leqslant 1, 0 \leqslant \phi < 2\pi$.

For a circle, actions are given by [17]:

$$I_\phi = p_\phi, \tag{32}$$

$$I_r = \pi^{-1}\sqrt{E}(\sqrt{1 - I_\phi^2/E} - (I_\phi/\sqrt{E})\cos^{-1}(I_\phi/\sqrt{E})), \tag{33}$$

where $m = 1/2$, and p_ϕ, E are angular momentum and energy, which are conserved.

The dependence $I_r(I_\phi)$ with $H = E = const$, as expressed by Eq.(33) is a level line (Fig.7). It is seen, that $I_r/\sqrt{E}$ is energy-independent function of

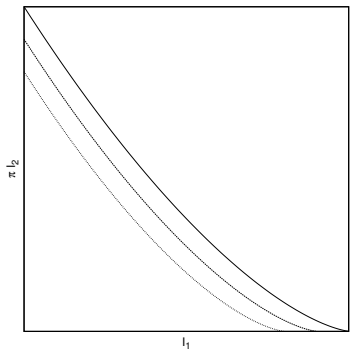

Figure 6: Level lines for Hamiltonian of a circle are obtained by scaling a line for energy 1.

$I_\phi/\sqrt{E}$, thus all level lines are obtained by simply scaling any of them in two directions. The curvature does not change sign, and tends to infinity for $I_\phi \to 1$. This corresponds to stability of whispering gallery modes against circle distortions. The condition for periodic trajectory is that a derivative dI_r/dI_ϕ in Eq.(33) is a rational number, which gives:

$$\cos^{-1}(p_\phi/\sqrt{E}) = \pi l/m. \tag{34}$$

The Laplace operator eigenfunctions for a unit disk with a Dirichlet boundary condition are:

$$f_{n,p}(r,\varphi) = \beta_{n,p} J_n(a_{n,p} r) \exp(in\varphi), \tag{35}$$

where J_n are Bessel functions, and $a_{n,p}$ their zeroes. Normalizing constants $\beta_{n,p}$ are calculated with scalar products of Bessel functions by themselves. Corresponding Laplace operator eigenvalues are $\mu^0_{n,p} = a^2_{n,p}$.

To obtain conditions for periodic trajectory in terms of Bessel functions, it is necessary to place in Eq.(34) eigenvalues of corresponding operators, which are n for angular momentum, and $a_{n,p}$ for square root of energy. Thus the periodic trajectory condition is:

$$n/a_{n,p} \approx \cos(\pi l/m). \tag{36}$$

This condition also can be derived directly from well known asymptotic of large order Bessel function [18]:

$$J_n(n/\cos\gamma) \sim \frac{\cos(n(\tan\gamma - \gamma) - \pi/4)}{\sqrt{\frac{1}{2} n\pi \tan\gamma}}. \tag{37}$$

The Bessel function zeroes close to 1000 are shown in Fig.7. The picture clearly demonstrates arcs similar to those obtained for a case of rectangle. Their positions agree with a condition of Eq.(36). Note, that in comparison with the rectangular resonator, the arc direction is inverted. This reflects the fact, that surfaces $H = const$ have different signs of curvature for two cases. The equations

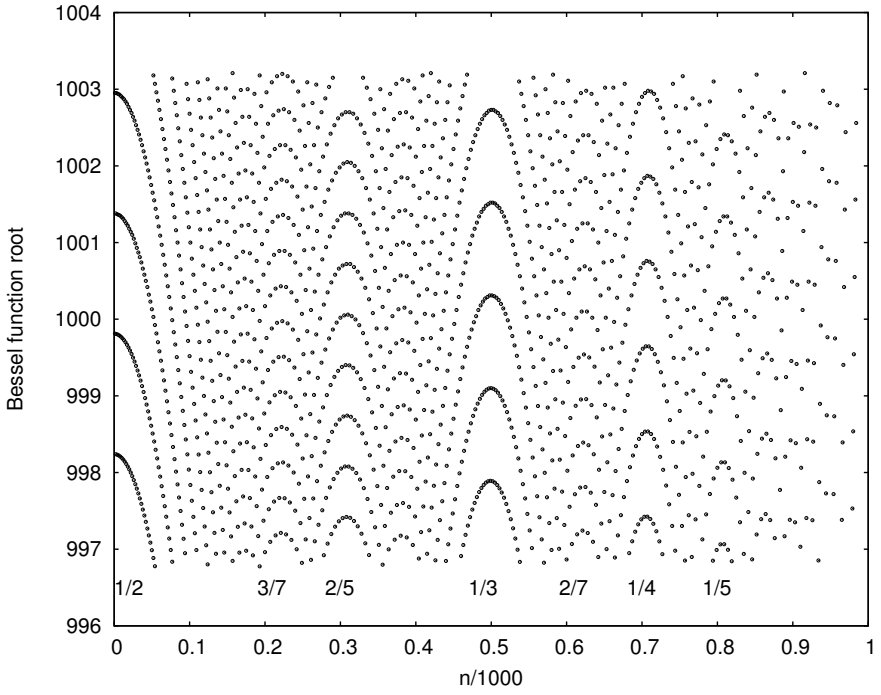

Figure 7: Bessel function zeroes close to 1000 for different function orders.

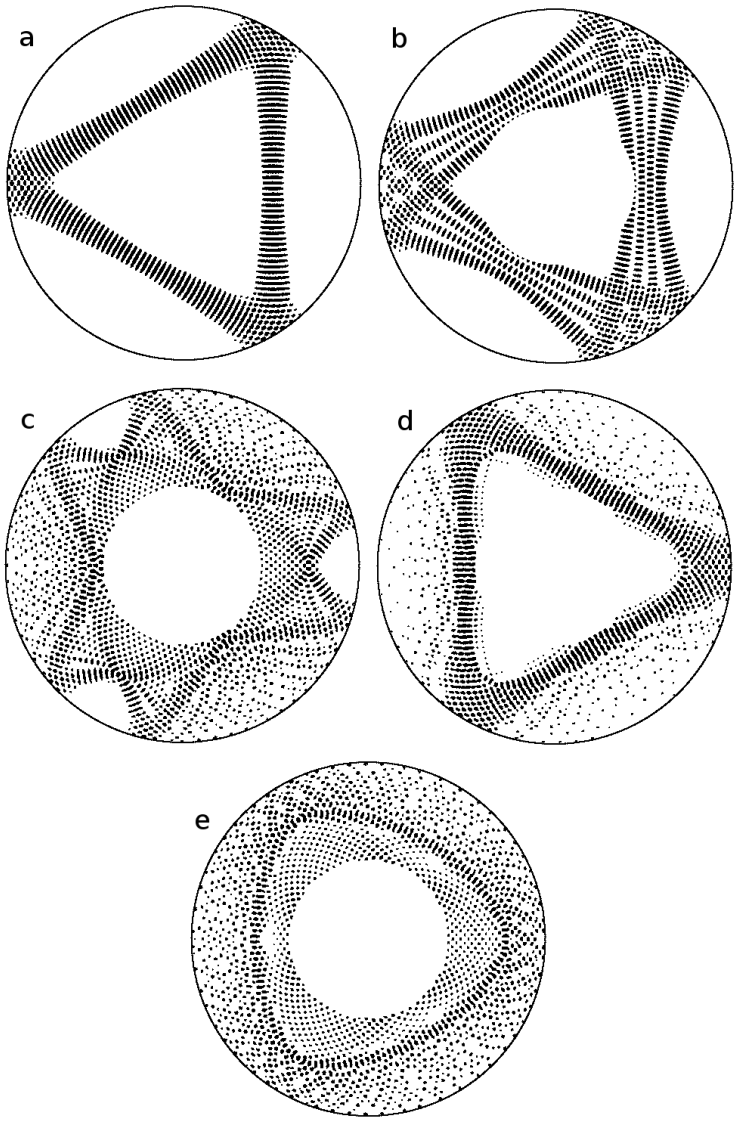

Figure 8: Examples of g functions of Eq.(41) in a circle for $d = 50, m = 3$ and central Bessel function with $n_0 = 100, a_{n_0,p_0} \sim 200$ ($p_0 = 22, a_{n_0,p_0} = 199.82150...$). The real part is shown, where it is bigger than a certain threshold. a.) The lowest eigenvalue $N = 0$ gives Gaussian beam around a stable periodic trajectory. b.) The $N = 3$ eigenvalue gives Hermite function profile. c.) The $N = 14$ eigenvalue produces a caustic. d.) The $N = 18$ eigenvalue corresponds to a condition $\lambda' \approx 2d$, it gives a scar mode along an unstable periodic trajectory.e.) For $N = 23$ the solution begins to approximate a cylindrical harmonic, though the 3-rd order symmetry is still seen.

for arc parameters α can be obtained either from Hamiltonian, by calculating curvatures, or directly from the Eq.(37).

The relevant conformal mapping is:

$$w(z) = z + \sum_{m=1}^{\infty} c_m z^{m+1}. \tag{38}$$

The perturbation for one term with real c_m is a multiplication by $-2\mu^0(m+1)c_m \cos(m\phi)r^m$.

It is easy to see, that to the first order in $|c_m|$ the boundary Γ is given by

$$r(\phi) = Re(1 + \sum_{m=1}^{N} c_m \exp(im\phi)). \tag{39}$$

Thus, by performing a Fourier transform one can reconstruct c_m coefficients if the shape of weakly distorted circle is known.

The perturbation matrix for only one term c_m in the vicinity of resonance has the same three diagonal structure, as for the case of a square.

$$\begin{aligned} &\langle f_{n1,p1}|P|f_{n2,p2}\rangle = \\ -2c_m(m+1)\mu^0 &\int_0^1 \beta_{12} J_{n1}(a_{n1,p1}r) J_{n2}(a_{n2,p2}r) r^{m+1} dr \times \\ &\int_0^{2\pi} exp(i(n2-n1)\varphi) cos(m\varphi) d\varphi, \end{aligned} \tag{40}$$

with $\beta_{12} = \beta_{n1,p1}\beta_{n2,p2}$. The angular part of this integral differs from zero only if $n1 = n2 \pm m$, as it was for the square, but radial part is not expressed in elementary functions. However, if $|p1 - p2| \ll p1, p2$, these integrals do not depend strongly on $p1 + p2$, as for the rectangular case. Thus,

$$g^{\lambda}(r,\phi) = \sum_{k=-\infty}^{\infty} \psi_k^{\lambda} \beta_{n0+km,p0-kl} J_{n0+km}(a_{n0+km,p0-lk}r) exp(i(n_0+km)\varphi). \tag{41}$$

0.7 Correspondence to KAM trajectories

Classically resonant KAM chaos regions of the phase space under perturbation c_m develop around resonant trajectories. The analysis of the previous section shows, that the perturbation produces in resonant regions the characteristic cylindrical harmonic superpositions of the form Eq.(41).

In a sense of quantum mechanics, ψ_k means a probability amplitude of having a cylindrical harmonic with $(n+km, p-kl)$ index, which classically corresponds to a trajectory with a characteristic angle γ deviated from exactly resonant value according to $\Delta cos(\gamma) \approx km/a_{n,p}$, since a values in the arc change slowly around the maximum. Thus, ψ_k coefficients describe the angular spectrum of the corresponding classical trajectory.

For low ψ_k eigenvectors we basically have Hermite functions. For small ν these are smooth and diminish rapidly with $|k|$. Close to the circle boundary $r \approx 1$, radial Bessel functions can be considered as cosine functions with similar spatial frequencies, and the principal contribution to the $\Psi(r, \phi)$ for $r \to 1$ in function of ϕ is a Fourier transform of ψ_k. Since a Fourier transform of Hermite function is again a Hermite function, for low eigenvalues we obtain modes localized at a circumference with respect to ϕ angle. In a classical sense the bundle of trajectories close to a stable periodic trajectory is obtained. Examples of such functions for $m = 3$ are shown in Fig.8, a,b.

For higher eigenvalues still corresponding to the condition $\lambda' < |2d|$, higher Hermite functions emerge. Close to the boundary they are weakly localized away from the stable periodic trajectory, and caustics appear, Fig.8c.

Classically, the trajectories in a phase space for $\lambda' < |2d|$ correspond to elliptic trajectories in the phase space of the KAM chaotic region - they are localized with respect to ϕ, γ angles. The $\lambda' \approx |2d|$ condition gives typical angular spectrum to which perturbation spreads :

$$\Delta n / a_{n,p} \sim |c_m)|^{1/2} sin(\gamma). \tag{42}$$

Thus, the perturbed region in the phase space extends to the angular range $\Delta\gamma \sim c^{1/2}$ which is a well known result on a KAM chaos.

For $\lambda' > |2d|$, and $\delta \neq 0$ the trajectories which are localized either for $k > 0$ or $k < 0$ are obtained. In the limit of big eigenvalues they correspond to perturbed single cylindrical harmonics, and demonstrate only weak localization at a boundary (Fig.8e).

The $\lambda' \approx |2d|$ region is an intermediate between these two types of behaviour.The localization there is stronger, than for $\lambda' < |2d|$ region - the function behaves as $(\Delta\phi)^{-1/2}$ close to the unstable periodic trajectory. For eigenvalues close to $|2d|$, scar modes are observed (Fig.(8d)). As we see, in this region the relative eigenvalue spacing for big d diminishes to zero, thus higher orders of perturbation theory, as well as corrections to first order operator, which we neglected for this analysis, will most strongly mix unperturbed cavity functions here. Thus, we are induced to identify these functions as participating in a classic homoclinic tangle. Note also, that the number of these functions, which have level separation lower, than some ε scales according to a known result on the homoclinic tangle extension.

The case of c_2 corresponds to the elliptic resonator, for which the exact solution is known. This exact solution also includes Mathieu equation for a radial part. Thus, for a single perturbation term c_m the resulting structures are related to those for an elliptical resonator.

0.8 Elliptical cavity

The case of ellipse is more complicated, and we consider it only briefly. Elliptic coordinates naturally appear within conformal mapping framework. Consider a function

$$w = a \cosh(z), \tag{43}$$

defined on the rectangle $0 < x \leqslant L_x, 0 < y \leqslant 2\pi$. Real and imaginary parts are:

$$u = a\cosh(x)\cos(y) \tag{44}$$

$$v = a\sinh(x)\sin(y), \tag{45}$$

which gives usual expressions for elliptic coordinates. The Eq.(43) maps the rectangle onto the inner part of the ellipse, the side $x = 0$ is projected onto a cut between foci. The Laplace operator Eq.(2) in these coordinates becomes

$$-\triangle f = \mu(\cosh(2x) - \cos(2y))f, \tag{46}$$

and it is separable, $f(x, y) = F_x(x)F_y(y)$. The equations for angular part $F_x(x)$ and radial part $F_y(y)$ are Mathieu and modified Mathieu equations,

$$\frac{d^2F_y}{dy^2} + (\kappa - 2q\cos(2y))F_y = 0 \tag{47}$$

$$\frac{d^2F_x}{dx^2} - (\kappa - 2q\cosh(2x))F_x = 0 \tag{48}$$

where $\mu = 2q$, and κ is separation constant. The solution of Mathieu equation has to be 2π periodic; for a given q this gives a set of possible κ values. The eigenvalue is fixed with a boundary condition for F_x and continuity across a cut (see [13, 14] for details).

A simple conformal map can be constructed in a form of Taylor series of Eq.(38). General theorems ensure that a smooth boundary perturbation produces a rapidly converging series. However, calculation of perturbation matrix elements in this case will require 2D integrals over the ellipse.

It is possible reduce the problem of finding an appropriate conformal mapping to the maps, which slightly deform a rectangle, $\omega(z)$. The ellipse distortion can be then obtained by applying the transformation of Eq.(43) $\cosh(\omega(z))$. Since x variable is cyclic, terms $\exp(mz)$ are involved. The map, that does not produce a discontinuity in $|w'|^2$ across a cut has a form

$$\omega(z) = z + \sum_{m=1}^{\infty} c_m \sinh(mz), \tag{49}$$

and c_m are complex coefficients. Consider, that only $c_m \neq 0$. For real c_m, the $x = L_x$ side is displaced in x - direction according to $c_m \sinh(mL_x)\cos(my)$. For purely imaginary $c_m = id$, the displacement is $-d\cosh(mL_x)\sin(my)$. Note, that in this case all four sides of the rectangle are distorted, and the cut between the foci is no more straight. However, the derivative absolute value is continuous across a cut.

It is seen, that if the boundary displacement in elliptic coordinates in known, $x(y) = L_x + d(y)$, then coefficients c_m can be determined by Fourier transform, similar to the case of a circle.

Calculation of perturbation matrix elements is then reduced to the estimation of four 1D integrals.

The Hamiltonian for elliptical billiard, action variables, and correspondence of classical and quantum mechanical solutions are discussed in detail in [13, 14]. The important difference with a circular case is that for elliptical billiard two types of movement are possible. One type is similar to a movement in a circle:

the trajectory do not cross the line between the foci, and the caustic is an ellipse. For another type, the trajectory passes between the foci after every collision with a boundary, and the caustic is hyperbolic. In the action plane I_1, I_2 two regions are seen, divided by a straight line $I_2 = \eta I_1$, and the transition across the line is not continuous. For two regions the curvature of a level line has different signs, and it tends to infinity when the common boundary is approximated from either side. On the other hand, for a correct semiclsssical approximation the square lattice in the vicinity of of a transition line become distorted as well [14]. Thus, the discussed approximation cannot be built in the vicinity of the classic trajectories passing close to the foci - special consideration is required there. These trajectories under perturbation form a homoclinic tangle in a phase space. If the initial periodic trajectory is far from this region, the Hill equation potential can be found, though for simple perturbation the matrix includes more than one diagonal. Numerics demonstrate, that if states far from dividing line are considered, the matrix elements diminish rapidly with $|k_1 - k_2|$, and the spectrum becomes wider if we approach the dividing line.

0.9 Relation to numerical solution

To illustrate the application of the method, we show here the eigenvalue calculation for the slightly distorted unity circle. We study the arc, which has a maximal eigenvalue equal to 10624.00 for $n = 50$, corresponding to $m = 3$. The conformal mapping function is $w(z) = z + 0.01z^4$. The numerical calculation of eigenmodes and eigenvalues for distorted circle is made with a freely distributed "FreeFem++" package based on the finite element method, with a mesh of approximately 200000 triangles. To build the perturbation matrix, 14 circle eigenmodes are taken around the maximal one, their eignvalues are given by the Bessel function roots. The off-diagonal elements of the Eq.(40) are estimated at the central eigenvalue. For $K \approx 100$, the semiclassical approximation is not very good, in particular the perturbation matrix coefficient vary 20 percent from one edge of the arc to another. We could not work with higher K values because of finite element software limitations. However, the sequence of modes similar to those of the Figure 5 is easily identified, except for a scar mode Fig.5d, which is not seen because of a small K number. We compare eigenvalues for 10 higher modes. The first Hermite-Gauss mode (Fig.6a) has a calculated eigenvalue 10807 ± 2, the approximation gives 10804. For the fourth mode (Fig.6b) we obtain 10603 and 10609, the sixth mode (Fig.6c) has 10448 and 10451, and the tenth (Fig.6d) has 10322 and 10324 values respectively. For the rest of modes, the results are similar. The error of the finite element method was estimated by calculating eigenmodes of the circle. The error is due to a finite mesh, but making a finer mesh resulted in program instability. It is seen, that the method gives a reasonable approximation even for the case not very close to a semiclassical one.

0.10 Discussion and conclusions

The results have close relationship to the initial stages of KAM chaos development in slightly distorted regular billiard. The wave structures corresponding

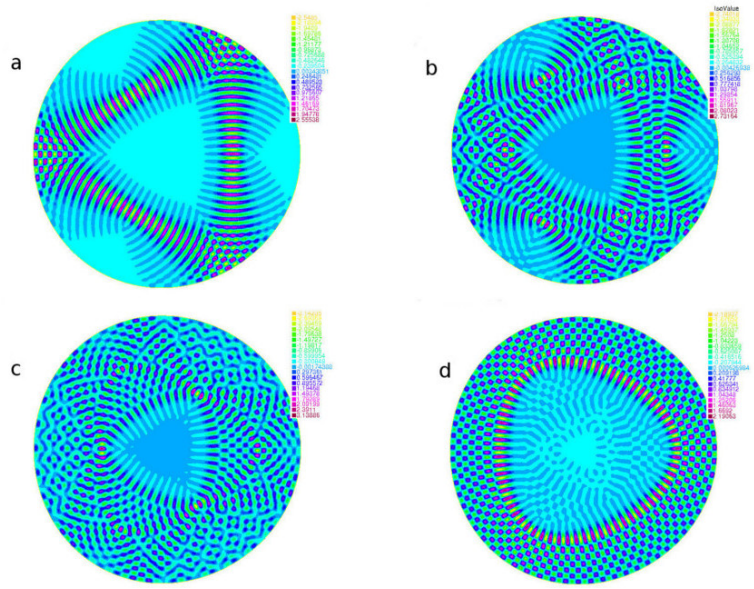

Figure 9: Numerically calculated eigenmodes in a slightly distorted circle, which correspond to the breaking of the single arc.

to initial stages of KAM chaos in ray optics are obtained. In fact, the reported construction seems natural for investigation of classical behaviour of trajectories, and their characteristic features, such as splitting. We do not consider these questions here in detail. However, keeping in mind this correspondence is useful for predicting the character of solutions. The relation to KAM chaos also makes estimations of validity range for approximations a laborious task.Since the typical perturbations include to some extent higher harmonics, thus modes corresponding to trajectories with big periods can become distorted in complicated ways. Higher perturbation terms also become quite involved. The validity range probably has to be investigated independently for each particular case.

The advantage of the approach is that it gives in a unified way different types of modes observed in cavities: nearly regular ones, semiclassical modes around stable trajectories, and scar modes. The last type is especially difficult for analytic methods. The approach also seems to be potentially useful for modes corresponding to a classical KAM homoclinic tangle, which is a question not completely understood now.

The appropriate object to study the modes related to homoclinic tangle is obtained by a small deformation of an ellipse. There the calculation of modal structure is made by simultaneously solving Mathieu and modified Mathieu equations, which is necessary to satisfy the boundary conditions. From this, parameters κ, q of Eqs.(47,48) are determined. The homoclinic tangle is observed when $\kappa \approx 2q$. In this case, the behaviour of solutions for big q is not trivial. The eigenvalues in function of some appropriately chosen quantum number lie on curves similar to those depicted in Fig.3a, but there exist two branches, one for symmetrical, and another for anti-symmetrical solutions. The eigenvalue spacing diminishes around the singular point where $\kappa \approx 2q$, but this dimin-

ishing is logarithmic, thus very big mode numbers are necessary to adequately represent the situation in a semiclassical limit. Though the curvature of lines $H(I_1, I_2) = const$ close to the singular point tends to infinity, the lattice of Fig.2 cannot be considered as a rectangular one there. Taking into account the interplay between level lines and curved lattice, the conditions of Fig.2 in a critical region become such, that the relative curvature in fact diminishes in this region to nearly zero for big q values. Thus, one can expect, that higher resonances, corresponding to big m, l numbers can become excited. For this it is also necessary that the corresponding perturbation matrix elements are big enough for m value in question. Though for circle the shape perturbation by a single low harmonic results in only one non-zero element, the calculation demonstrates, that for the case of ellipse close to a singular region, a relatively big number of matrix elements is non-zero. The numerics suggests, that this number is logarithmically growing with q, but appropriate estimations are still under investigation.

Bibliography

[1] Korneev, N. *Cogent Physics* **2016**, accepted.

[2] Reichl,L., *The Transition to Chaos: Conservative Classical Systems and Quantum Manifestations*; Springer: New York, 2004.

[3] Cao, H.; Wiersig, J. *Rev. Mod. Phys.* **2015**, *87*,61–111.

[4] Harayama T., Shinohara S. *Laser and Photonics Reviews* **2011**, *5(2)*, 247–271.

[5] Dubertrand, R., Bogomolny, E., Djellali, N., Lebental, M., Schmit, C. *Phys. Rev. A* **2008**, *77*, 013804.

[6] Bruno, O.P., Reitich, F. *Jour. Fourier Anal. Appl.* **2001**, *7*, 171–189.

[7] Chakraborty, S., Bhattacharjee,J.K, Khastgir S.P. *Journal of Physics A: Mathematical and Theoretical* **2009**, *42 (19)*, 195301.

[8] Tureci, H., Schwefel, H., Stone, A., Narimanov, E. *Optics express* **2002**, *10 (16)*, 752–776.

[9] Schinzinger, R., Laura, P.A.A *Conformal Mapping: Methods and Applications*; Dover Publications, 2003.

[10] Leonhardt, U. *Science* **2006**,*312*, 1777–1780.

[11] Reck, K., Thomsen, E.V., Hansen, O. *Optics express* **2011**,*19 (3)*, 1808–1823.

[12] Berry, M.V., Tabor, M.*Proc.R. Soc. London* **1976**,*A349*, 101–123.

[13] Waalkens, H., Wiersig,J., Dullin H.R. *Annals of physics* **1997**,*260 (1)*, 50–90.

[14] Sieber, M. *J. Phys. A* **1997**, *30*, 4563–4596.

[15] Itin, A. P., Neishtadt, A.I. *Regular and Chaotic Dynamics* **2003** *8.1*, 59–66.

[16] Li, W., Reichl, L.E., Wu, B. *Phys. Rev. E* **2002**, *65*, 056220.

[17] Ree, S., Reichl, L.E. *Physical Review E* **1999**, *60(2)*, 1607 .

[18] Watson, G.N. A Treatise on the Theory of Bessel Functions; 2nd.ed., Cambridge University Press, 1966.